Journal Pre-proof

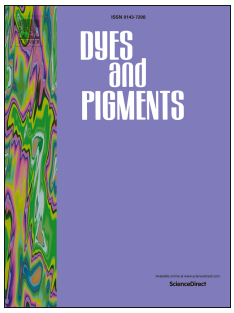

(*E*)-2-Styrylanthracene-9,10-dione: A new type of fluorescent probe core and its application in specific mitochondria imaging

Xu Zhang, Ting-jian Zhang, Zhao-ran Wang, Qiu-yin Wang, Peng-fei Lu, Hai-yang Zhao, Lin Wang, Fan-hao Meng

PII: S0143-7208(21)00663-X

DOI: https://doi.org/10.1016/j.dyepig.2021.109797

Reference: DYPI 109797

To appear in: *Dyes and Pigments*

Received Date: 24 July 2021

Revised Date: 24 August 2021

Accepted Date: 6 September 2021

Please cite this article as: Zhang X, Zhang T-j, Wang Z-r, Wang Q-y, Lu P-f, Zhao H-y, Wang L, Meng F-h, (*E*)-2-Styrylanthracene-9,10-dione: A new type of fluorescent probe core and its application in specific mitochondria imaging, *Dyes and Pigments* (2021), doi: https://doi.org/10.1016/j.dyepig.2021.109797.

Author Contributions:

Xu Zhang: Methodology, Original Draft Writing; **Ting-jian Zhang**: Conceptualization, Review and Editing; **Zhao-ran Wang**: Investigation and Data analysis; **Qiu-yin Wang**: Validation; **Peng-fei Lu**: Synthesis; **Hai-yang Zhao**: Instrument resources; **Lin Wang**: Review and Editing; **Fan-hao Meng**: Project administration.

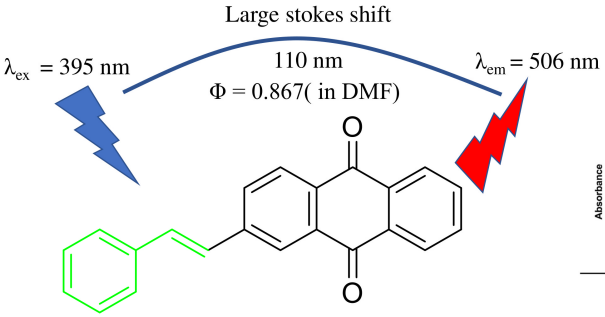

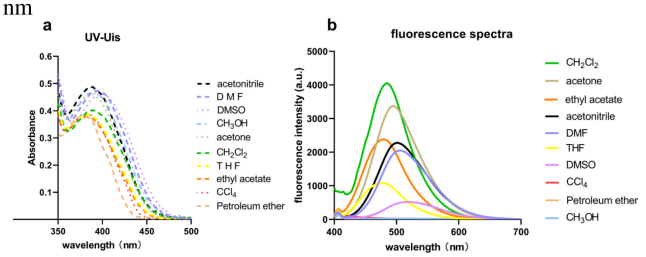

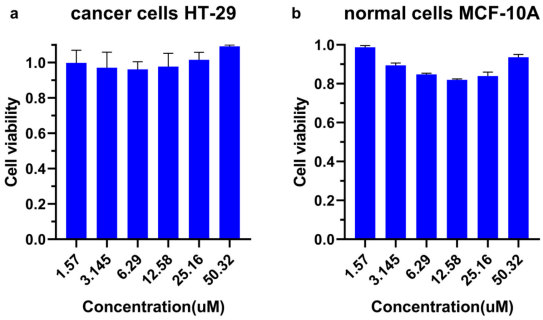

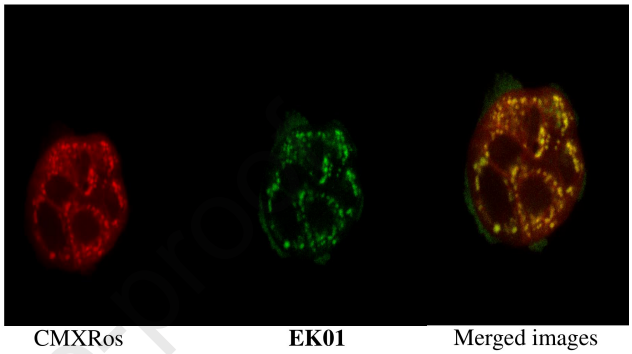

CMXRos **EK01** Merged images

(*E*)-2-styrylanthracene-9,10-dione: a new type of fluorescent probe core and its application in specific mitochondria imaging

Xu Zhang [a, 1], Ting-jian Zhang [a, 1], Zhao-ran Wang [a], Qiu-yin Wang [a], Peng-fei Lu [a], Hai-yang Zhao [b], Lin Wang [a], Fan-hao Meng [a, *]

[a] *School of Pharmacy, China Medical University, 77 Puhe Road, North New Area, Shenyang 110122, China*

[b] *Teaching Center for Basic Medical Experiment, China Medical University, 77 Puhe Road, North New Area, Shenyang 110122, China*

*Corresponding author.

E-mail: fhmeng@cmu.edu.cn (F. H. Meng).

[1] These two authors contributed equally to this work.

Abstract

Herein, a new type of fluorescent probe core, (*E*)-2-styrylanthracene-9,10-dione (**EK01**), was developed which displayed strong fluorescence quantum yield (Φ = 0.867 in DMF; Φ = 0.561 in acetone; Φ = 0.616 in CH_2Cl_2; Φ = 0.265 in DMSO), good photostability, large stokes shift (90 nm to 120 nm) and molar extinction coefficients (0.5875 × 10^4 - 0.7609 × 10^4 $mol^{-1}\cdot L\cdot cm^{-1}$). During cell assays and co-localization experiments, **EK01** showed excellent cell membrane permeability and low cytotoxicity against MCF-10A (human mammary epithelial cell line) and HT-29 (human colorectal adenocarcinoma cell line). Particularly, we surprisingly discovered that **EK01** could selectively aggregate in mitochondria and specific stain it in a green emissive fluorescent form, which means that **EK01** could be a real-time specifically monitor of mitochondria in living cells with a high signal-to-noise ratio. Hence a new mitochondria imaging method was established which is incubating **EK01** with living cells for 1 h at a final concentration of 6 ~ 12 μM, then visualizing under a confocal microscope at 395 nm. It is worth noting that the

fluorescence efficiency of **EK01** is not outstanding in organisms, it has much stronger fluorescence efficiency in other organic solvent systems (such as DMF, acetone and CH_2Cl_2). Therefore, as a new type of fluorescent core that is easy to synthesis and graft, we believe that (*E*)-2-styrylanthracene-9,10-diones have the potential to develop a variety of fluorescence platforms applying in different fields.

Keywords: Fluorescent probe; (*E*)-2-Styrylanthracene-9,10-dione; Mitochondrial imaging.

1. Introduction

Organic small molecule fluorescent probes have become valuable tools in a variety of related research fields, including physics, chemistry and life science, and played important roles in food safety detection, environmental monitoring, medical diagnosis and pharmacological and toxicological analyses, due to their high sensitivity and selectivity, tunable excitation and emission wavelengths, and customizable functionalization structure modification [1-5]. In recent years, fluorescent probes based on xanthene, coumarin, and BODIPY are currently used, some of which are commercially available [6-10]. But to meet the demands of fluorescent probes for changing rapidly bioanalytical applications, research and development of more new fluorescent probes with good fluorescence spectrum characteristics is still the key and core of the development of fluorescence analysis technology.

Traditional bio-detection methods include radioisotope labeling, microscopy, and electrochemistry, but the radioisotope labeling method has the risk of radiation and with the arrival of the half-life, the detection signal will be greatly reduced; the microscopy observation method cannot be effective for the observation of specific biological activity due to the limitation of

magnification; and electrochemical monitoring easily damages biological samples. As the result of these drawbacks, the traditional bio-detection methods have been greatly limited in practical applications. Compared with traditional bio-detection methods, fluorescence analysis technology has become one of the most important methods of biological detection now and had great practical application because of its advantages such as non-hazard, rapid and intuitive analysis, high sensitivity, and friendly operating environment [11-14]. Due to its advantages, fluorescence analysis technology can be applied not only to mice, but also to biological tissues or living cells to perform cell fluorescence coloring, to realize in-situ detection and real-time monitoring for the content and spatial distribution of the measured substance in the biological tissues or cells [15-17]. Ultimately, fluorescence imaging technology can achieve the visual observation of cell morphology, structure, and life activity.

Anthraquinone is a traditional fluorescent core [6,7]. In our previous research, we accidentally found that some anthraquinone synthetic intermediates possess explicit fluorescent phenomenon [18]. Driven by the curiosity, subsequently, we screened an in-house chemical library of anthraquinones and fortunately identified (*E*)-2-styrylanthracene-9,10-dione (**EK01**). **EK01** exhibited strong fluorescence under an ultraviolet lamp at the excitation wavelength of 312 nm (**Fig.S1**), obviously demonstrating that it's a new type of fluorescent core with a unique chemical structure. In the present work, we described the synthesis method, spectrophotometric properties, cytotoxicity and fluorescence quenching of **EK01**, especially, its application in specific mitochondria imaging in living cells was developed.

2. Experimental section

2.1. Synthesis

The synthetic route of **EK01** was outlined in **Scheme 1**. Using phthalimide and toluene as starting materials, 2-(4-methylbenzoyl)benzoic acid (**1**) was synthesized via a Friedel-Crafts acylation, which was further cyclized to afford 2-methylanthracene-9,10-dione (**2**). Bromination of intermediate **2** provided 2-(bromomethyl)anthracene-9,10-dione (**3**), which then treated with triphenyl phosphorus to yield 2-((triphenyl-λ5-phosphanylidene)methyl)anthracene-9,10-dione (**4**). Finally, **EK01** was successfully synthesized via a classical Wittig reaction. According to the high coupling constant of double bond hydrogens (J = 16.3 Hz) in ^{1}H NMR spectrum, the double bond configuration of **EK01** was identified as *E*-form (or *trans*-form). The synthetic procedure of intermediates **1**, **2** and **3** had been described in our previous work [18].

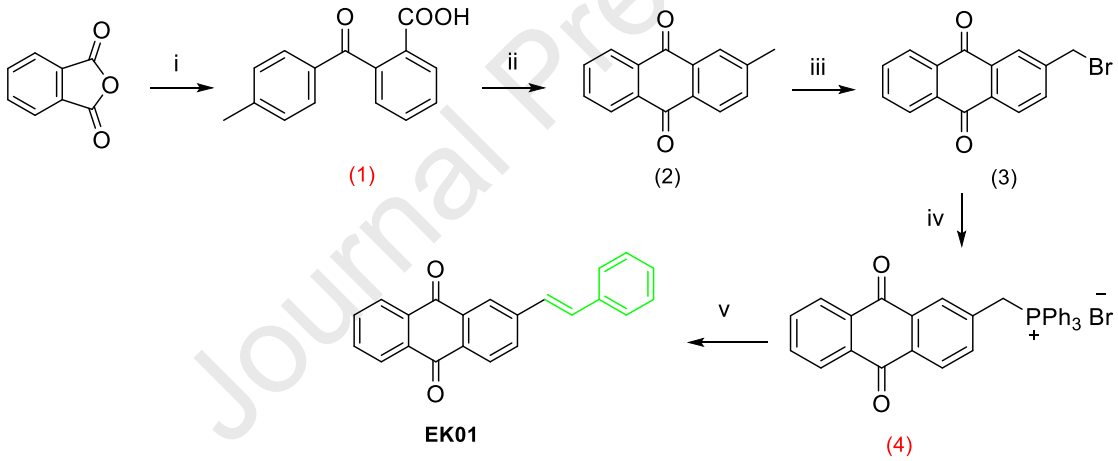

Scheme 1 Synthetic route of **EK01.** Reagents and conditions: (i) toluene, anhydrous $AlCl_3$, 50°C, 4 h; (ii) conc. H_2SO_4, 100□, 1 h; (iii) *N*-bromosuccinimide, benzoyl peroxide, CCl_4, refluxed for 24 h Pd/C; (iv) triphenylphosphine, CH_2Cl_2, refluxed for 6 h; (v) benzaldehyde, $(Et)_3N$, CH_2Cl_2, room temperature for 12 h.

2.1.1. Preparation of 2-((triphenyl-λ^5-phosphanylidene)methyl)anthracene-9,10-dione (4)

A mixture of **3** (0.5 g, 1.7 mmol) and triphenylphosphine (0.65 g, 2.5 mmol) in CH_2Cl_2 (30 mL) was stirred and refluxed for 6 h. The reactive mixture which had been taken out and spin-dried in ethyl acetate (40 mL) was refluxed at 60℃ for 30 min, then cooled, filtered and dried to obtain **4**

(0.42 g, 45.16%) as a yellow powder which was used directly in the next step.

2.1.2. Synthesis of (*E*)-2-styrylanthracene-9,10-dione (EK01)

A mixture of **4** (0.42 g, 0.83 mmol), benzaldehyde (0.075 g, 0.71 mmol) and triethylamine (0.17 g, 1.7 mmol) in CH_2Cl_2 (6 mL) was stirred at room temperature for 12 h. The reactive mixture was added in H_2O (30 mL) and CH_2Cl_2 (30 mL) and the organic layer was extracted, vacuum distillation and silica gel column chromatography (ethyl acetate: petroleum ether = 1:20) to obtain **EK01** (0.133 g, 50.53%) as a yellow powder. ^{1}H NMR (600 MHz, DMSO-d_6) δ 8.30 (s, 1H), 8.23 – 8.14 (m, 3H), 8.10 (d, J = 7.9 Hz, 1H), 7.91 (m, 2H), 7.70 (d, J = 7.4 Hz, 2H), 7.54 (d, J = 16.3 Hz, 1H), 7.47 (d, J = 16.5 Hz, 1H), 7.41 (t, J = 7.3 Hz, 2H), 7.33 (t, J = 7.1 Hz, 1H) [19]. ^{13}C NMR (150 MHz, DMSO-d_6) δ 182.54, 181.92, 143.14, 136.36, 134.59, 134.41, 133.54, 133.17, 133.08, 132.77, 131.62, 131.52, 131.44, 128.81, 128.62, 127.48, 127.16, 126.76, 126.70, 124.57. HRMS (ESI) *m/z* $[M+H]^+$ calcd. for $C_{22}H_{15}O_2$: 311.10720, found: 311.10516.

2.2. Spectrophotometric Measurements

The UV-vis measurements (UV-2100 spectrophotometer, UNICO) were performed in different solvents (CH_2Cl_2, CCl_4, DMSO, DMF, THF, CH_3CN, MeOH, acetone, ethyl acetate, petroleum ether) with the concentration of 64.4 μM. The fluorescence measurements (F-7100 Fluorescence Spectrophotometer, HITACHI) were performed in the above-mentioned solvents with a concentration of 6.29 μM. The fluorescence of the probe in DMF-H_2O and DMSO-H_2O with different proportions was measured. The absorption spectra were recorded at 350-475 nm. The fluorescent emission spectra were recorded at 475-750 nm with an excitation wavelength at 395 nm. The viscosities of DMF-H_2O and DMSO-H_2O with different proportions were measured at the same temperature as the relevant fluorescence spectra.

Fluorescence quantum yields (Φ) of **EK01** in a variety of solvents were measured by using quinine sulfate dihydrate in 0.1 mol/L sulfuric acid solution (Φ = 0.54) as standard. The measurements of fluorescence quantum yields have been made using the "comparative method", which the standard equation is given below [20,21].

$$\Phi_x = \Phi_{ST}\left(\frac{k_x}{k_{ST}}\right)\left(\frac{\eta_x^2}{\eta_{ST}^2}\right) \quad (A \leq 0.05)$$

In the formula, Φ_{ST} is the fluorescence quantum yield of the standard substance, k_X and k_{ST} are the slopes of the linear fitting line of the test substance and the standard substance, respectively, and η_X and η_{ST} are the refractive indices of the test substance and the standard substance, respectively.

2.3. Cell cytotoxicity

The cell cytotoxicity was detected by MTT assay on MCF-10A cells (human mammary epithelial cell line) and HT-29 cells (human colorectal adenocarcinoma cell line). The cells were cultured in a 96-well plate for 24 h and then incubated with different concentrations of **EK01** (0 - 50 μM) for 24 h. Then, 10 μL MTT (10 mg/mL) was added and incubated for 4 h at 37°C. The nutrient solution was removed slowly and 100 μL DMSO was added into the 96-well plate which finally was shaken for 10 min. The absorbance intensities at 490 nm were measured by the microplate reader. All the experiments were repeated three times, and the data were expressed as the percentage of control cells.

2.4. Cell imaging assay

To demonstrate the fluorescence imaging capability of **EK01**, HT-29 cells were used for cell imaging under a confocal laser scanning microscope. The cells were seeded in a glass-bottom petri dish and incubated with 5% CO_2 at 37°C for 24 h. The probe was then dissolved in DMSO at 3.22

μmol/mL and diluted with a DMEM medium to obtain the desired concentration. The final concentration of DMSO in the medium was less than 1%.

3. Results and discussion

3.1. UV-vis Absorption and Fluorescence Emission

3.1.1. Optical properties of EK01

The absorption spectra and emission spectra of **EK01** in the different solvents were shown in **Fig. 1** and the optical properties were tabulated in **Table1**. The UV-vis absorption of **EK01** exhibited the absorption maximum in the range of 380 – 399 nm with molar extinction coefficients (ε) at around 0.5875×10^4 - 0.7609×10^4 $mol^{-1} \cdot L \cdot cm^{-1}$. The absorption maximum displayed obvious red-shift in polar solvents, such as DMSO (at 399 nm) and DMF (at 395 nm), compared with in non-polar solvent petroleum ether (at 380 nm). Besides, **EK01** displayed strong fluorescence quantum yield in a variety of solvents as displayed in **Table 1**. The emission wavelengths were ranging from 477.4 nm to 529.6 nm. It was worth pointing out that **EK01** possesses large stokes shift (91.4 – 149.6 nm) in all the tested solvents. In addition, the photostability assay revealed that the fluorescence intensity of **EK01** only weakly reduced over a long irradiation time of 24 h, suggesting that **EK01** has high photostability (**Fig.S5**).

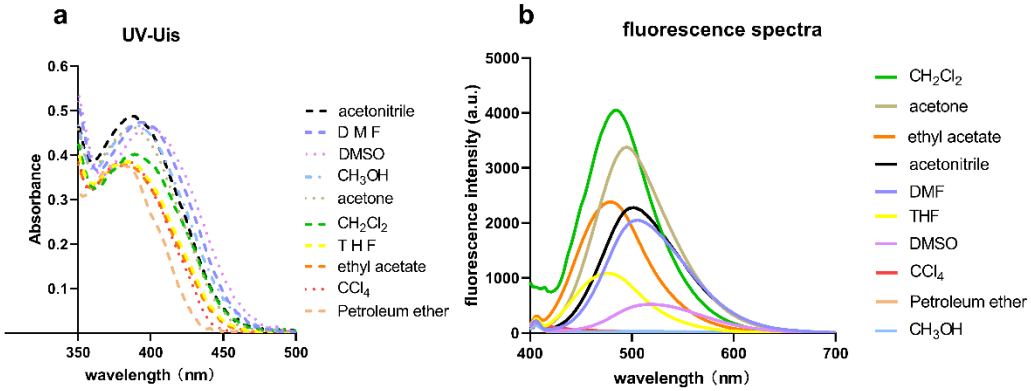

Fig. 1 (a) The absorption spectra and (b) fluorescence emission spectra of **EK01** in the different solvents.

Table 1 optical properties of **EK01** in the different solvents.

Solvent	λ_{max}(exc)[ab]	ε[c]	λ_{max}(em)[a]	Intensity(λ_{em})	Stokes shift	Φ
DMF	395	7391	506	2051	111	0.867
DMSO	399	7203	517	521	118	0.265
THF	386	6031	477	1083	91	0.602
Acetone	386	7234	495	3376	109	0.561
CH_2Cl_2	389	6281	484	4050	95	0.616
CH_3OH	389	7313	507	26	118	NA [d]
Petroleum ether	380	5875	530	10	150	NA
CCl_4	383	6015	NA	NA	NA	NA
Acetonitrile	389	7609	501	2279	112	0.767
Ethyl acetate	383	5906	479	2383	96	0.343

[a]λ values in nm. [b]λ_{max}(exc) for direct excitation of the fluorescence. [c]($mol^{-1}\cdot L\cdot cm^{-1}$). [d] experimental data cannot be measured.

3.1.2. Viscosity Dependence Study

The effect of viscosity on the fluorescence emission of **EK01** was investigated. As depicted in **Fig. 2**, the fluorescence intensity increased with increasing organic phase volume fraction separately in DMF/H_2O and DMSO/H_2O mixed solvents. To study the relationship of viscosity and fluorescence intensity, the fluorescence emission spectra at 505.6 nm (DMF/H_2O) and 516.8 nm (DMSO/H_2O) were measured at room temperature, meanwhile, the corresponding viscosities of **EK01** in the two mixed solvent systems were tested. The values of both the fluorescence intensity and the viscosity were converted into natural logarithmic form. As shown in **Fig. 2b**, the corresponding plots of ln (fluorescence intensity) – ln (viscosity) exhibited great linear relationship (Adj.R^2 = 0.9901 in DMF/H_2O, Adj.R^2 = 0.9901 in DMSO/H_2O). The results suggested that **EK01** could act as a viscosity indicator.

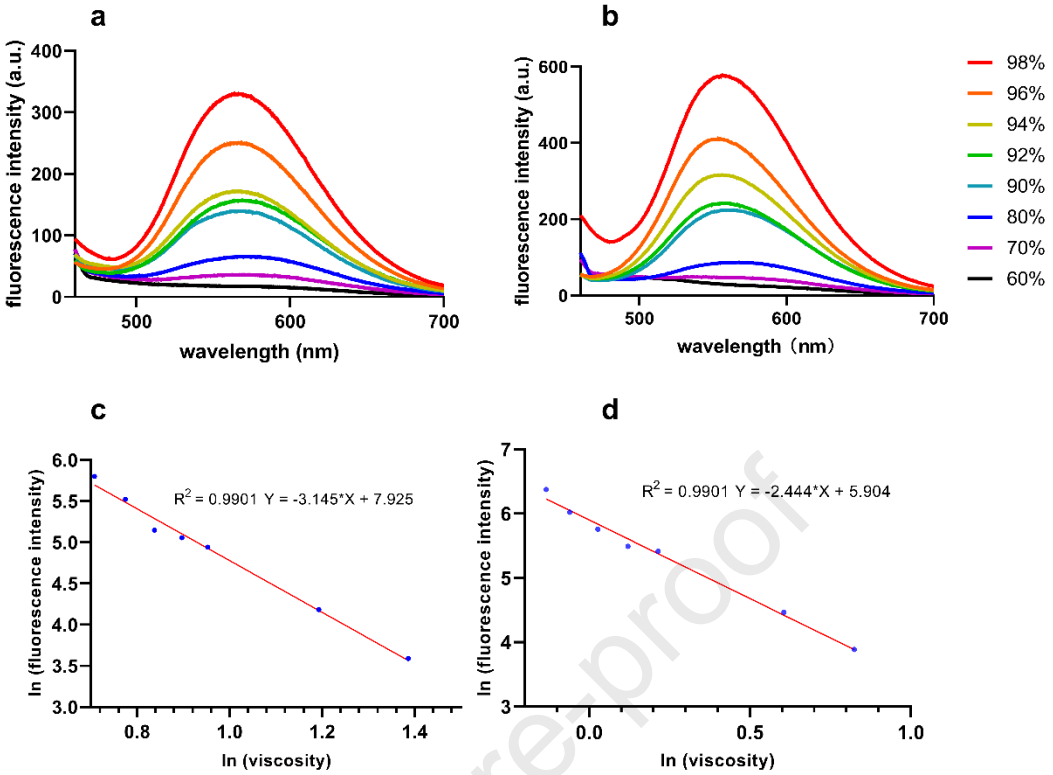

Fig. 2 The fluorescence emission spectra of **EK01** (a) in DMSO/H_2O mixtures and (b) in DMF/H_2O mixtures; Plot of natural logarithm of the fluorescence intensity and the natural logarithm of the viscosity (c) in DMSO/H_2O mixtures and (d) in DMF/H_2O mixtures.

3.1.3. Fluorescence Quenching mechanism

During spectroscopy experiments, it had found that **EK01** has much weaker fluorescence in protic solvents (such as methanol and water) than in non-protic solvents (such as DMF, DMSO and CH_2Cl_2). Meanwhile, when a small amount of water (less than 2%) existed, **EK01** showed a rapid decrease in fluorescence intensity in both DMF and DMSO solutions (as depicted in **Fig. 3**). This phenomenon is difficult to explain by viscosity dependence as mentioned above, but is consistent with intramolecular charge transfer (ICT) mechanism. It is known that ICT fluorescent probes are shown to be environmentally sensitive due to the formation of ITC excited states, which means that in hydrophobic, the probes exhibit strong fluorescence, however, in highly polar solvents, the probes

have only weak fluorescence [22,23]. **EK01**, as a typical ITC fluorescent probe with large conjugate system, we speculated that its fluorescence quenching mechanism in the presence of a small amount of H_2O may be caused by the vibrational deactivation via hydrogen bond [22]. As shown in **Fig. 4**, the water molecules could form hydrogen bonds with the carbonyl groups of the anthraquinone core, so that producing a strong solvation effect. This opens a way for fluorescence inactivation. The similar fluorescence quenching channel was also reported on some UV stabilizers [22].

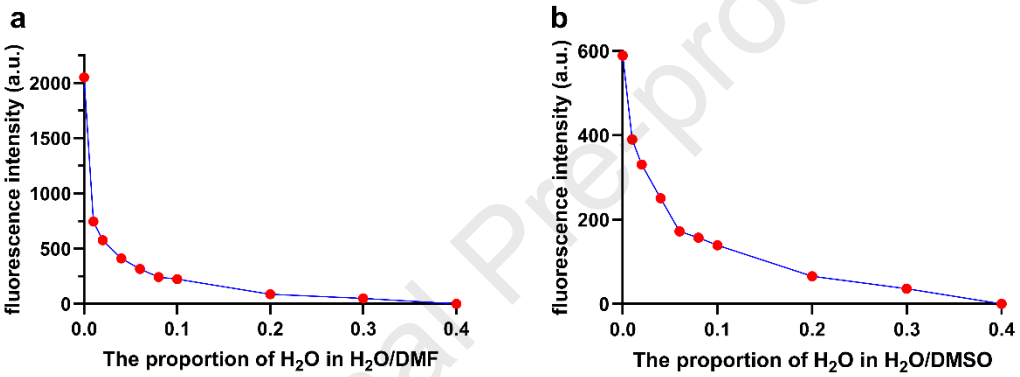

Fig. 3 The change of fluorescence intensity depended on H_2O proportion. (a) in DMF/H_2O mixtures and (b) in DMSO/H_2O mixtures.

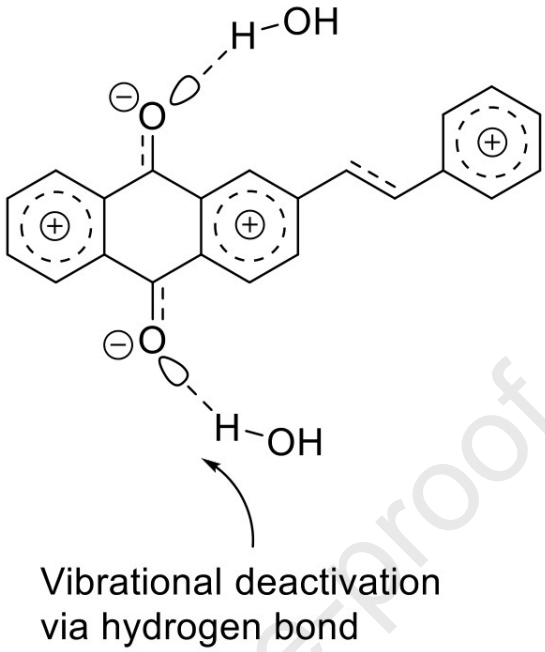

Fig. 4 Hydrogen-bond donation to **EK01** from protic solvents.

3.2. Cytotoxicity Assay

Cytotoxicity was evaluated by the standard MTT assay in the two types of cell lines (MCF-10A healthy cells line and HT-29 cancer cells line) to quantify cell viability after treated with different concentrations of the probe. **Fig. 5** clearly indicated that the viability of both cell lines decreased along with the increase of the three relatively low concentrations (1.57, 3.145, 6.29 μM). Nevertheless, the viabilities were more than 85% in both MCF-10A cells and HT-29 cells after 24 h of incubation with **EK01**, which means that **EK01** only possesses a slight cytotoxic effect on cells. Interestingly, the cell survival rate increased at high concentrations of 25.16 μM and 50.32 μM. This phenomenon can be explained by the physical aggregation of **EK01** at high concentrations, resulting in a decrease in dissolved **EK01**. In summary, **EK01** is a safe cell staining agent, which will few

affect the survival of cells under staining conditions.

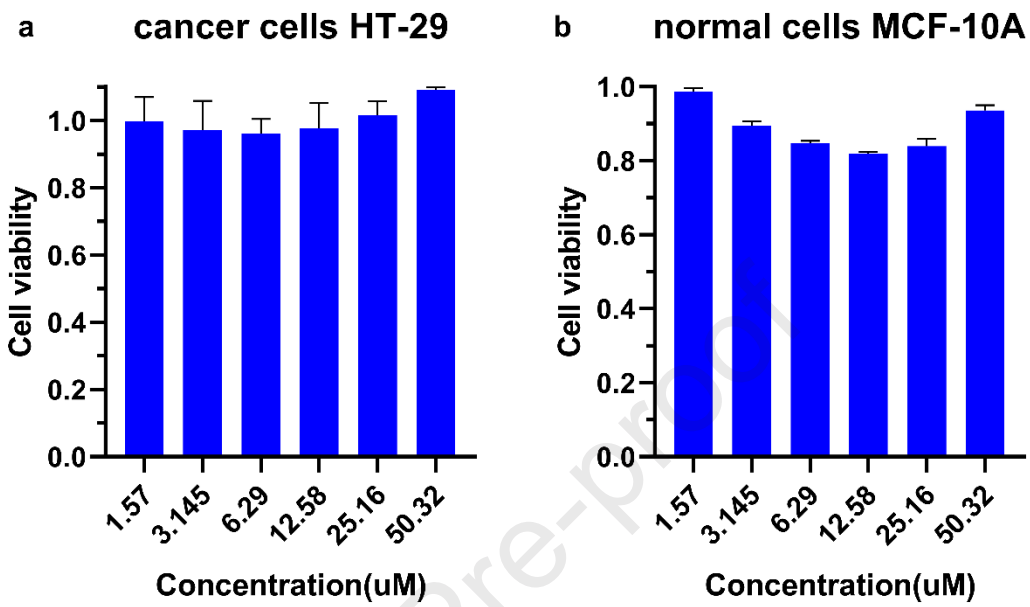

Fig. 5 MTT assay of (a) HT-29 cell and (b) MCF-10A were treated in the presence of **EK01** (1.57, 3.145, 6.29, 12.58, 25.16, 50.32 μM) and incubated for 24 h.

3.3. Imaging Assay

Firstly, we interestingly observed that **EK01** possessed apparent green fluorescence staining phenomenon for HT-29 cells under an inverted fluorescence microscope (**Fig.S6**). In order to obtain higher resolution images and to better delineate the area around the subcellular structure of HT-29 cells, we proceeded to co-localization experiments with **EK01** and other commercial organelles dyes under a confocal microscopy. The preliminary studied surprisingly found that **EK01** seemed to be extremely specific for mitochondria, but had no response to other organelles, such as nucleus, cell membrane and endoplasm (**Fig. S7**). To accurately confirm the mitochondria localization of **EK01**, co-localization investigations of **EK01** and a commercial deep-red mitochondrial tracker (CMXRos) were performed. As shown in **Fig. 6c**, **f**, **i**, **l**, the merged images clearly indicated that

the green staining images of **EK01** and the red staining images of CMXRos perfectly coincided, forming merged orange patterns. These results, clearly demonstrated that **EK01** is a specific mitochondria probe for living cell imaging, and its specificity and imaging ability for mitochondria are equivalent to CMXRos. Besides, **Fig.6b**, **e**, **h**, **k** showed that the fluorescence intensity revealed a concentration-dependent increase in the concentration range of 6.29 ~ 25.16 μM. When the concentration of **EK01** reached 6.29 μM, a good green visual rendering effect can be achieved, meeting the needs of dyeing (**Fig. 6b**). Meanwhile, the resolution of the image will not be significantly improved when the concentration is higher than 25.16 μM. In short, co-localization assay proved that **EK01** is a green specific mitochondria probe for living cells, and its staining concentration is recommended between 6 ~ 12 μM.

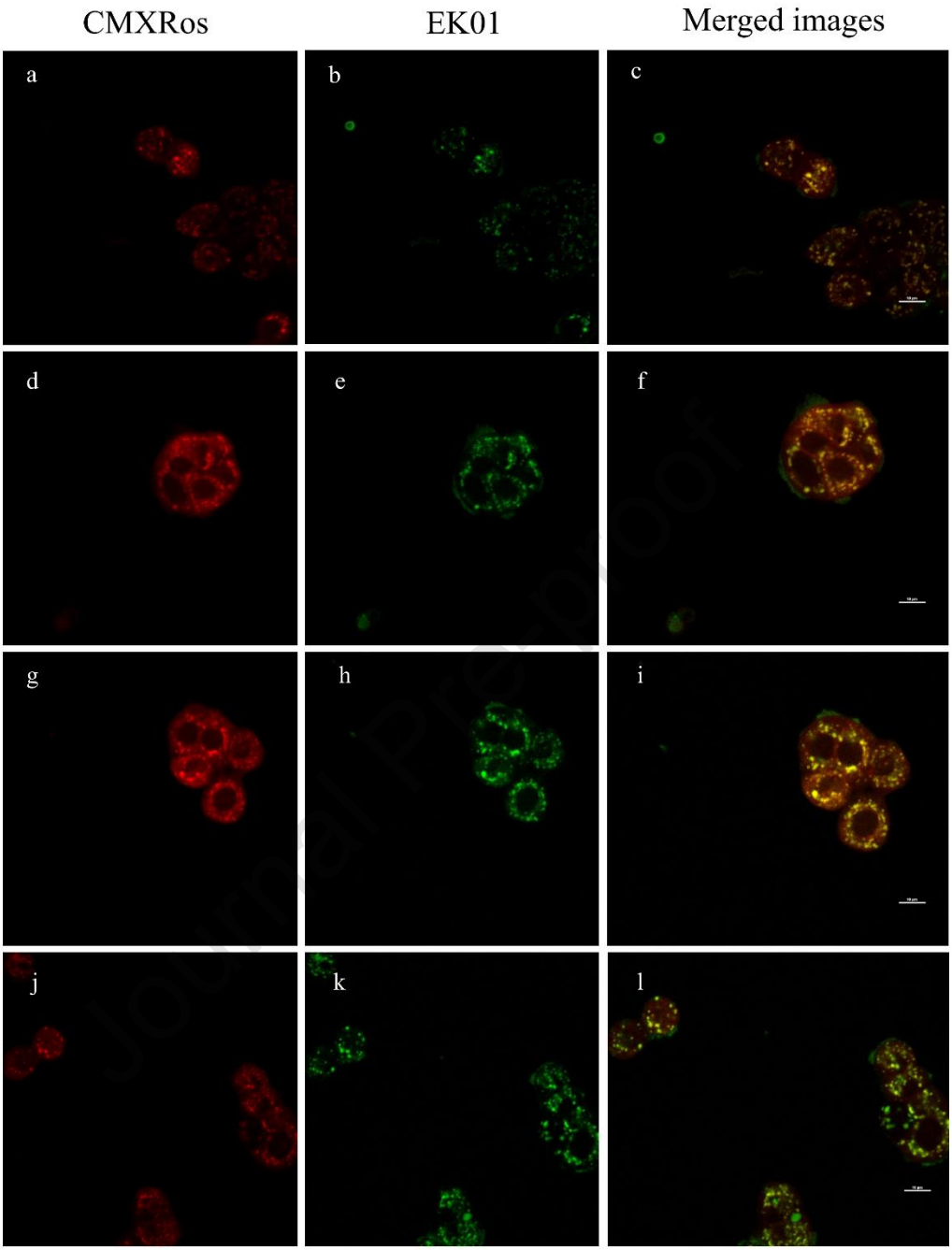

Fig. 6 Confocal fluorescence images of HT-29 cells stained with CMXRos (3 μM) and **EK01** (6.29 μM, 12.58 μM, 25.16 μM, 50.32 μM). Column 1: CMXRos (a, d, g, j; red channel: λ_{ex} = 579 nm, λ_{em} =599 nm). Column 2: **EK01** (b, e, h, k; green channel: λ_{ex} = 395 nm, λ_{em} =500 nm). Column 3: Merged images (c, f, i, l). Scar bar: 10 μm.

In the following study, we investigated the influence of incubation time for the stain. Two time

points of 30 min and 1 h were set, and the result was illustrated in **Fig. 7**. As shown in **Fig. 7c**, **d**, **g**, **h**, the staining results of 30 min and 1 h were all excellent at highly concentrations of 25.16 μM and 50.32 μM, implying that these concentrations may already be higher than the optimum concentration required for dyeing. Furthermore, as shown in **Fig. 7a**, **b**, **e**, **f**, the fluorescence intensities emerged an obviously time-dependent improvement at relatively low concentrations of 6.29 μM and 12.58 μM. After 30 min of incubation, the fluorescence intensities at 6.29 μM and 12.58 μM were both too weak to image, correspondingly, the imaging results were excellent after 1 h staining under same concentrations. The time-dependent stain manner suggested that **EK01** needed to take a certain time to stain or specific accumulate in mitochondria.

In summary, the staining result of 1 h was better than that of 30 min at low concentrations. And after 1h incubation time, the increase in concentration had little effect on the outcome of staining for cells. Finally, based on the cytotoxicity and imaging assays, an **EK01** based special mitochondria imaging method was suggested which is incubation of **EK01** with living cells for 1 h at a final concentration of 6 ~ 12 μM.

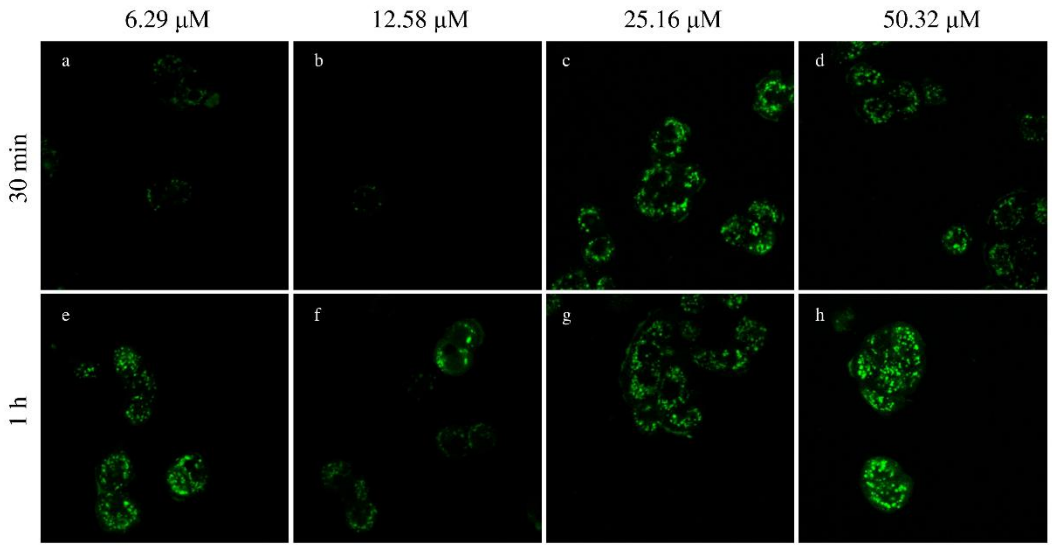

Fig. 7 Confocal fluorescence images in HT-29 cells stained with **EK01** at the four concentrations for 30 min and 1h incubation time.

4. Conclusions

In summary, a novel type of fluorescent probe core, (*E*)-2-styrylanthracene-9,10-dione (**EK01**), was discovered. A series of advantages including strong fluorescence quantum yield, good photostability, large stokes shift, high molar extinction coefficients and well biocompatibility, implies its potential to be widely applied in numerous fields. The facile and highly efficient synthetic method based on a Wittig reaction ensures the reliable access of **EK01** and its derivatization. In addition, using **EK01** as a green staining agent for living cells, a new specific mitochondria imaging method was established with high signal-to-noise ratio and low-cytotoxicity. Other applications of **EK01** and its derivatives are under exploration.

Declaration of competing interests

The authors declare that they have no known competing financial interests or personal relationships that could have appeared to influence the work reported in this paper.

Acknowledgements

This work was supported by the National Natural Science Foundation of China (Grant No. 81803355) and Young Talents Program of China Medical University.

5. References

[1] Chan, J., Dodani, S. C., & Chang, C. J. (2012). Reaction-based small-molecule fluorescent probes for chemoselective bioimaging. *Nature chemistry*, *4*(12), 973–984. https://doi.org/10.1038/nchem.1500

[2] Dong, B., Song, X., Wang, C., Kong, X., Tang, Y., & Lin, W. (2016). Dual Site-Controlled and Lysosome-Targeted Intramolecular Charge Transfer-Photoinduced Electron Transfer-Fluorescence Resonance Energy Transfer

Fluorescent Probe for Monitoring pH Changes in Living Cells. Analytical chemistry, 88(7), 4085–4091. https://doi.org/10.1021/acs.analchem.6b00422

[3] Kraayenhof, R. , Visser, A., & Gerritsen, H. C. (2003). Fluorescence spectroscopy, imaging and probes : new tools in chemical, physical and life sciences. Journal of Microscopy, 212(2), 212-213. https://doi.org/10.1046/j.1365-2818.2003.01255.x

[4] Jiang, B., Wei, Y., Xu, J., Yuan, R., & Xiang, Y. (2017). Coupling hybridization chain reaction with dnazyme recycling for enzyme-free and dual amplified sensitive fluorescent detection of methyltransferase activity. Analytica Chimica Acta, 949(Complete), 83-88. https://doi.org/10.1016/j.aca.2016.11.003

[5] Li, M., Feng, W., Zhai, Q., & Feng, G. (2017). Selenocysteine detection and bioimaging in living cells by a colorimetric and near-infrared fluorescent turn-on probe with a large stokes shift. Biosensors & bioelectronics, 87, 894–900. https://doi.org/10.1016/j.bios.2016.09.056

[6] Chen, X., Zhou, Y., Peng, X., & Yoon, J. (2010). Fluorescent and colorimetric probes for detection of thiols. Chemical Society reviews, 39(6), 2120–2135. https://doi.org/10.1039/b925092a

[7] Du, J., Hu, M., Fan, J., & Peng, X. (2012). Fluorescent chemodosimeters using "mild" chemical events for the detection of small anions and cations in biological and environmental media. Chemical Society reviews, 41(12), 4511–4535. https://doi.org/10.1039/c2cs00004k

[8] Kamkaew, A., Lim, S. H., Lee, H. B., Kiew, L. V., Chung, L. Y., & Burgess, K. (2013). BODIPY dyes in photodynamic therapy. Chemical Society reviews, 42(1), 77–88. https://doi.org/10.1039/c2cs35216h

[9] Mittapalli, R. R., Namashivaya, S., Oshchepkov, A. S., Kuczyńska, E., & Kataev, E. A. (2017). Design of anion-selective PET probes based on azacryptands: the effect of pH on binding and fluorescence properties. Chemical communications (Cambridge, England), 53(35), 4822–4825. https://doi.org/10.1039/c7cc01255a

[10] Kolemen, S., & Akkaya, E. U. (2017). Reaction-based bodipy probes for selective bio-imaging. Coordination

Chemistry Reviews, 354. https://doi.org/10.1016/j.ccr.2017.06.021

[11] Chan, J., Dodani, S. C., & Chang, C. J. (2012). Reaction-based small-molecule fluorescent probes for chemoselective bioimaging. Nature chemistry, 4(12), 973–984. https://doi.org/10.1038/nchem.1500

[12] Terai, T., & Nagano, T. (2013). Small-molecule fluorophores and fluorescent probes for bioimaging. Pflugers Archiv : European journal of physiology, 465(3), 347–359. https://doi.org/10.1007/s00424-013-1234-z

[13] Tang, Y., Lee, D., Wang, J., Li, G., Yu, J., Lin, W., & Yoon, J. (2015). Development of fluorescent probes based on protection–deprotection of the key functional groups for biological imaging. Chemical Society Reviews, 44(15), 5003–5015. https://doi.org/10.1039/c5cs00103j

[14] Chen, H., Tang, Y., & Lin, W. (2016). Recent progress in the fluorescent probes for the specific imaging of small molecular weight thiols in living cells. Trends in Analytical Chemistry: TRAC, 76, 166–181. https://doi.org/10.1016/j.trac.2015.11.014

[15] Kushida, Y., Nagano, T., & Hanaoka, K. (2015). Silicon-substituted xanthene dyes and their applications in bioimaging. The Analyst, 140(3), 685–695. https://doi.org/10.1039/c4an01172d

[16] Lee, M. H., Kim, J. S., & Sessler, J. L. (2015). Small molecule-based ratiometric fluorescence probes for cations, anions, and biomolecules. Chemical Society reviews, 44(13), 4185–4191. https://doi.org/10.1039/c4cs00280f

[17] Lee, M. H., Kim, J. S., & Sessler, J. L. (2015). Small molecule-based ratiometric fluorescence probes for cations, anions, and biomolecules. Chemical Society reviews, 44(13), 4185–4191. https://doi.org/10.1039/c4cs00280f

[18] Zhang, T. J., Li, S. Y., Yuan, W. Y., Wu, Q. X., Wang, L., Yang, S., Sun, Q., & Meng, F. H. (2017). Discovery and biological evaluation of some (1H-1,2,3-triazol-4-yl)methoxybenzaldehyde derivatives containing an anthraquinone moiety as potent xanthine oxidase inhibitors. Bioorganic & medicinal chemistry letters, 27(4), 729–732. https://doi.org/10.1016/j.bmcl.2017.01.049

[19] Djukic, B., & Perepichka, D. F. (2012). Unexpected formation of a cyclic vinylene sulfate in the synthesis of

ethynyl-substituted acenes. Chemical communications (Cambridge, England), 48(53), 6651–6653. https://doi.org/10.1039/c2cc32805d

[20] Williams, A., Winfield, S. A., & Miller, J. N. (1983). Relative fluorescence quantum yields using a computer-controlled luminescence spectrometer. Analyst, 108(1290), 1067-0. https://doi.org/10.1039/AN9830801067

[21] Crosby, G. A. , & Demas, J. N. (1971). Measurement of photoluminescence quantum yields. j phys chem. Journal of Physical Chemistry, 75(8), 31-31. https://doi.org/10.1021/j100678a001

[22] de Silva, A. P., Gunaratne, H. Q., Gunnlaugsson, T., Huxley, A. J., McCoy, C. P., Rademacher, J. T., & Rice, T. E. (1997). Signaling Recognition Events with Fluorescent Sensors and Switches. Chemical reviews, 97(5), 1515–1566. https://doi.org/10.1021/cr960386p

[23] Wu, D., Sedgwick, A. C., Gunnlaugsson, T., Akkaya, E. U., Yoon, J., & James, T. D. (2017). Fluorescent chemosensors: the past, present and future. Chemical Society reviews, 46(23), 7105–7123. https://doi.org/10.1039/c7cs00240h

Highlights

1. A novel fluorescent probe core (**EK01**) was developed for specific mitochondria imaging in living cells.
2. The probe shows massive stokes shift and high fluorescence quantum yield.
3. The probe shows excellent cell membrane permeability and low cytotoxicity.
4. The probe could real-time specifically monitor mitochondria for a long time.

Conflict of Interest

The authors declare that they have no known competing financial interests or personal relationships that could have appeared to influence the work reported in this paper.